Available online at www.sciencedirect.com
ScienceDirect
International Journal of Mass Spectrometry 255–256 (2006) 150–163
International Journal of Mass Spectrometry
www.elsevier.com/locate/ijms

# Dynamics of chemical and charge transfer reactions of molecular dications: VI Reactions of $C_4H_3^{2+}$ with Kr, Xe, $H_2$, $N_2$, NO, $NH_3$, $C_2H_2$, and $CH_4$

Juraj Jašik [1], Jana Roithová, Jan Žabka, Roland Thissen [2], Imre Ipolyi [1], Zdenek Herman *

*V. Čermák Laboratory, J. Heyrovský Institute of Physical Chemistry, Academy of Sciences of the Czech Republic, Dolejškova 3, 182 23 Prague 8, Czech Republic*

Received 22 November 2005; received in revised form 19 January 2006; accepted 20 January 2006
Available online 21 February 2006

**Abstract**

Reactions of the hydrocarbon dication $C_4H_3^{2+}$ with a series of atomic and molecular targets (Kr, Xe, $N_2$, NO, $NH_3$, $C_2H_2$, and $CH_4$) were investigated in crossed-beam scattering and guided-beam (quadrupole–octopole–quadrupole, QOQ) experiments. Non-dissociative charge transfer (NDCT), leading to the product ion $C_4H_3^+$, and proton transfer (PT), leading to the product ion $C_4H_2^+$, were observed. In several systems, however, dissociative charge transfer (DCT) contributed significantly to the formation of the product ion $C_4H_2^+$. Full scattering diagrams of the products $C_4H_3$ and $C_4H_2^+$ were obtained for the reaction with acetylene. For the other systems, energy profiles of the products close to the angular maximum were obtained. The hydrocarbon products $C_4H_2^+$ and $C_4H_3^+$ were scattered mostly forward, suggesting an impulsive mechanism of their formation at the collision energies investigated; the only exception was proton transfer with $H_2$, where the energy profile of $C_4H_2^+$ indicated substantial backward scattering and formation of an intermediate. From relative translational energy distributions of the products, conclusions could be made about electronic states of the hydrocarbon cations formed in these reactions.


*Keywords:* Reaction dynamics; Molecular dications; Charge transfer; Proton transfer

## 1. Introduction

Chemical reactions in encounters of multiply charged ions with atoms and molecules represent a much less explored area of chemical kinetics and dynamics than chemical reactions of singly charged ions. A handful of studies of chemical reactions of doubly charged atomic metal ions [1–5] have been augmented only about a decade ago by observation of chemical reactions of molecular dications [6]. Since that time, however, the number of studies of kinetics and dynamics of dication–molecule bond-forming reactions has been gradually increasing. Formation of chemical products and fragments resulting from them has been described in detail for reactions of molecular dications $M^{2+}$ ($CF_2^{2+}$ [6–9], $CF_3^{2+}$ [10], and $CO_2^{2+}$ [11]) with molecular hydrogen. The reaction products are usually two singly charged ions, $MH^+$ and a naked proton, of a rather high relative translational energy resulting from Coulomb repulsion, or their dissociation products. The chemical reaction is usually accompanied by a charge transfer process leading to $M^+$ and $H_2^+$ or to their dissociation products. Bond-forming reactions leading to a pair of products dication–neutral have been described, too [3,12,13]. A potential energy model was developed based on crossings of dication–neutral surfaces and Coulomb repulsion surfaces of two singly charged products [7,8]. The model rationalizes mutual competition of these processes and was successfully applied to a variety of systems [8,11,14,15].

In a recent study of reactions between the hydrogen-containing triatomic dication $CHCl^{2+}$ with $D_2$ [15–17] and Ar [18], the dynamics of facile proton transfer from the dication to the neutral reactant was described. The reaction represents the strongest reaction channel in the above-mentioned systems

* Corresponding author. Tel.: +420 2 6605 3514; fax: +420 2 8658 2307.
*E-mail address:* zdenek.herman@jh-inst.cas.cz (Z. Herman).
[1] Pre-Doctoral Stipendist under the auspices of the EU Network MCI (Generation, Stability and Reaction Dynamics of Multiply-Charged Ions), 2002–2003. Home address: Department of Experimental Physics, Comenius University, Bratislava, Slovak Republic.
[2] Post-Doctoral Stipendist under the auspices of the EU Network MCI (Generation, Stability and Reaction Dynamics of Multiply-Charged Ions), 2003. Home address: Laboratoire de Chimie Physique, UMR8000, CNRS-Université Paris-Sud, 91 405 Orsay, France.

1387-3806/$ – see front matter © 2006 Elsevier B.V. All rights reserved.
doi:10.1016/j.ijms.2006.01.028

(besides a less probable non-dissociative charge transfer and a chemical reaction leading to the $CHDCl^+$ formation in the reaction with $D_2$) and it is characterized by a strongly forward scattering of the product ion $CCl^+$. This suggests an impulsive, direct mechanism of the process. The reaction may be a rather general process in encounters of strongly acidic hydrogen-containing dications and neutral molecular bases. Proton transfer reactions have been earlier described in collisions of multiprotonated biomolecules, produced in electrospray ionization, with neutral gaseous bases [19], negative ions [20], or protonated fullerene dications and neutrals [21].

In an effort to pursue the dynamics of proton transfer reactions and its competition with other processes in different systems, we investigated the reactivity of the hydrocarbon dication $C_4H_3^{2+}$ with different neutral systems. Formation of the radical dication $C_4H_3^{2+}$ was observed in electron double ionization of a variety of aliphatic saturated and unsaturated hydrocarbons, where the dication represents one of the strongest doubly charged product ions [22]. Limited data on the structure and energetics of $C_4H_3^{2+}$ have been recently complemented by an experimental and theoretical study of the proton affinity of the diacetylene cation and calculations of the ground and excited states of both $C_4H_3^{2+}$ and $C_4H_3^+$ [23]. It appears that the dication $C_4H_3^{2+}$ is likely to belong among the thermodynamically stable molecular doubly charged ions [23,24].

In collisions of $C_4H_3^{2+}$ with different target molecules, three processes were observed occurring with different probabilities and leading to ion products $C_4H_3^+$ and $C_4H_2^+$: non-dissociative charge transfer (NDCT, electron exchange, electron transfer), dissociative charge transfer (DCT), and proton transfer (PT). The product $C_4H_2^+$ could be formed by the latter two processes. Initial internal excitation of the dication reactant $C_4H_3^{2+}$ turned out to be of decisive importance in the dissociative charge transfer. Relative probabilities of these processes were estimated using two different experimental methods. Measurements of product translational energy distributions provided information on the energetics of the processes. In reaction with acetylene, scattering diagrams of the product hydrocarbon ions were obtained.

## 2. Methods

### 2.1. Experiments

The experiments were carried out on the crossed-beam apparatus EVA II. The performance and application of this machine to this type of scattering experiments was described earlier [7,8,11,15]. Briefly, the dication $C_4H_3^{2+}$ was produced by impact of 130 eV electrons on butadiene in a low-pressure ion source. The ions were extracted, mass analyzed, and decelerated by a multi-element lens to the required laboratory energy. The $C_4H_3^{2+}$ beam was crossed at right angles with a beam of the target atoms (Kr and Xe) or molecules ($N_2$, NO, $NH_3$, $CH_4$, $C_2H_2$, and $C_2D_2$) emerging from a multichannel jet. The dication beam had an angular and energy spread of 1.2° and 0.5 eV (full-width-at half-maximum, FWHM), respectively. The collimated neutral beam had an angular spread of 6° (FWHM) and thermal energy distribution at 300 K. Reactant and product ions passed through a detection slit (2.5 cm from the scattering center) into a stopping potential energy analyzer. They were then accelerated and focused into a detection mass spectrometer, mass analyzed, and detected with the use of a dynode electron multiplier. Laboratory angular distributions were obtained by rotating the two beams about the scattering center. Modulation of the neutral beam and phase-sensitive detection of the ion products was used to remove background scattering effects.

Relative probabilities of observed processes were obtained from mass spectra of the $C_4H_3^+$ and $C_4H_2^+$ products measured at the angular maximum. Distributions of the relative translational energy of products were obtained from product ion translational energy measurements at the angular maximum or close to it.

To obtain scattering diagrams, a combination of laboratory angular distributions and energy profiles recorded at a series of laboratory scattering angles was used in the usual way. The contours in the scattering diagrams refer to the Cartesian probability distribution [25,26], normalized to the maximum in the particular scattering diagram. Relative translational energy distributions of the products, $P(T')$, were obtained by integration of the scattering diagrams in the usual way [25,26].

Complementary data on relative probabilities of processes in the studied systems were obtained from independent experiments using a different apparatus (later on referred to as QOQ experiments). The experiments were performed with the Berlin tandem SIFT–GIB apparatus [27], which consists of a multifunctional ion source, a selected ion flow tube (SIFT), and a quadrupole–octopole–quadrupole (QOQ) unit. In the present study, only the QOQ part was used as a regular guided-ion-beam mass spectrometer. For ionization, an additional electron-ionization source situated directly in front of the QOQ unit was used. The $C_4H_3^{2+}$ dications were formed by dissociative electron ionization of butadiene molecules and mass-selected by means of the first quadrupole. The reactions were conducted in the octopole reaction cell at two different nominal laboratory energies as defined by the voltage applied to the octopole ($U_{oct}$), while the pressure of the collision gas was kept in the order of $10^{-5}$ to $10^{-4}$ mbar. Products of the reactions were mass analyzed by means of the second quadrupole and detected. Data acquisition was done with the Merlin Automation Software (ABB Extrel). Usually, 50–150 scans were accumulated for a single spectrum, and 3–7 spectra were recorded for a given reaction to minimize the experimental error. The intensity of a signal ($I_i$) was determined by integration of the central part of the corresponding peak in order to avoid mass overlap and to simultaneously increase the accuracy of the measurements. The branching ratios between $C_4H_3^{2+}$ and $C_4H_2^{2+}$ as well as $MH^+$ and $M^+$ (M = Kr, Xe, NO, and $NH_3$) were derived as averages from the recorded mass spectra. The branching ratios discussed here were found to depend only modestly on the translational energy. The data were measured at nominal laboratory kinetic energies of the projectiles close to 0 and 50 eV, with an energy spread of ±10 to ±12 eV.

### 2.2. Calculations

The calculations were performed using the density functional method B3LYP [28,29] in conjunction with Dunning's correlation consistent triple zeta basis set (cc-pVTZ) [30–32] as implemented in Gaussian 98 [33]. For all the optimized structures, frequency analysis at the same level of theory was used in order to assign them as real minima. Energies of all stationary points were refined by the G2 method [34] using geometries optimized at B3LYP/cc-pVTZ level of theory.

## 3. Results and discussion

### 3.1. Energetics of the hydrocarbon species involved

The reactant dication $C_4H_3^{2+}$ is the most abundant dication formed by electron ionization of $C_4$ hydrocarbons [22]. The radical dication $C_4H_3^{2+}$ is rather an exception among these mostly closed-shell dications of the type $C_nH_{2m}^{2+}$ ($m$ = l–4). The most recent estimation, based on charge stripping experiments with $C_4H_3^+$ generated from butadiene [23] and corrected for the recently published IE of the toluene cation [35], used as a reference for the charge-stripping experiments, leads to the adiabatic ionization energy of the most stable open-chain structure, $(H_2C–C–C–CH)^{2+}$, $IE_a(C_4H_3^+ \rightarrow C_4H_3^{2+}) = 16.0 \pm 0.3$ eV. Based on the recent values of the heat of formation of $C_4H_2$, 4.81 eV [36], its proton affinity of 7.64 eV [37], and $\Delta_fH(H^+) = 15.858$ eV [38], the heat of formation of the cation is $\Delta_fH(C_4H_3^+) = 13.02$ eV. From this value and the above mentioned ionization energy of the cation, 16.0 eV, the heat of formation of the dication is $\Delta_fH(C_4H_3^{2+}) = 29.0 \pm 0.4$ eV. The proton affinity of the diacetylene cation $C_4H_2^+$ based on the experimental and theoretical data [23] and corrected on the basis of anew IE of the toluene cation [35] is positive and equal to $1.8 \pm 0.4$ eV. This makes the ground state of the dication $C_4H_3^{2+}$ stable with respect to a loss of a proton; all other conceivable dissociation asymptotes were found even more endothermic. Thus, the dication $C_4H_3^{2+}$ appears to add to the set of thermodynamically stable dications in the gaseous phase [23,24]. Because of the thermodynamic stability of the dication $C_4H_3^{2+}$ toward dissociation and of the expected barrier to its dissociation, the dication can be formed with a high initial internal energy. The height of the barrier toward dissociation to $C_4H_3^+ + H^+$ was estimated by analogy with a similar dissociation process $C_2H_2^{2+} \rightarrow C_2H^+ + H^+$, studied in detail both experimentally [39] and theoretically [40,41]. The barrier height was estimated as 2.0 eV. Thus, the initial internal energy of the dication $C_4H_3^{2+}$ may be as high as 3.8 eV (see Fig. 1). Another estimation [23], based on thermochemistry, gives a similar value of 3.6 eV. In view of the rather strong spontaneous and collision-induced dissociation observed in MS/MS studies of the dication [23], it is likely that a substantial fraction of the dications $C_4H_3^{2+}$ in our experiments was excited close to its dissociation limit (see a likely $P(E_{int})$ in Fig. 1, left). This is not surprising, as a rather violent double ionization and fragmentation process has to be invoked in the formation of the dication from butadiene, because three H atoms are ejected and

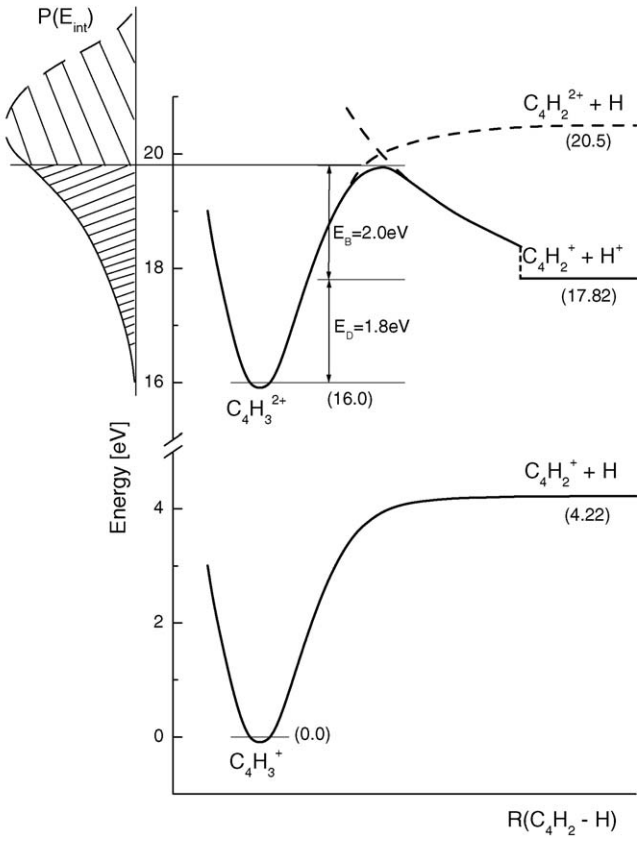


Fig. 1. Schematics of the potential energy curves for $C_4H_3^{2+}$ and $C_4H_3^+$; left: possible internal energy excitation of the dication, $P(E_{int})$.

the $C_4$-backbone is stretched to the linear configuration. The initial internal energy appears to be crucial in estimating the ratio of dissociative charge transfer versus proton transfer in the systems studied.

A series of isomers of the cation $C_4H_3^+$ was located at the B3LYP/cc-pVTZ level of theory [23]. The corresponding energies are listed in Table 1. For the linear open-chain structure $(H_2C–C–C–CH)^+$, the energies of the ground singlet state ($^1\mathbf{1}^+$) and the first excited triplet state ($^3\mathbf{1}^+$) were calculated. The dissociation energy of $C_4H_3^+$($^1\mathbf{1}^+$) to $C_4H_2^+ + H$ is 4.2 eV [23]. The triplet state ($^3\mathbf{1}^+$) lies 1.37 eV above the singlet state and has presumably the same dissociation limit. The relevant structures of the other isomers can be found in [23], they have no immediate importance for the discussion of the results of this paper. Low-lying excited states of the dication were calculated as a part of this study and they are also listed in Table 1. The most stable isomer ($^2\mathbf{1}^{2+}$) has the open-chain structure $(H_2C–C–C–CH)^{2+}$, analogous to the structure of the cation. Details about the structure of the other dication isomers are given in [23].

The heat of formation of the cation $C_4H_2^+$, $\Delta_fH$ $(C_4H_2^+) = 14.98$ eV, is slightly higher than the usual tabulated value [38], derived with the old value for $\Delta_fH$ of the neutral molecule $C_4H_2$. It is based on the ionization energy of diacetylene IE$(C_4H_2) = 10.17$ eV [42,43] and on the above mentioned recent value for the heat of formation of the neutral molecule, 4.81 eV [36]. Excited states of the diacetylene cation $C_4H_2^+$ were located in spectroscopic and electron spectroscopy stud-

Table 1
Energetics of the hydrocarbon species involved

| | $E_{ex}$ (eV)[a] | Designation, structure[b] | Note |
|---|---|---|---|
| $C_4H_3^{2+}$ | 0.00 | ($^2$**1**$^{2+}$)[a], but-3-yn-l-en-2 | $IE_a(C_4H_3^+) = 16.0 \pm 0.4$ eV[c], $\Delta_f H(C_4H_3^{2+}) = 29.0$ eV[d] |
| | 1.68 | ($^2$**2**$^{2+}$)[a] | |
| $C_4H_3^+$ | 0.00 | ($^1$**1**$^+$)[a], but-3-yn-l-en-2-yl | $\Delta_f H(C_4H_3^+) = 13.02$ eV[e] |
| | 1.37 | ($^3$**1**$^+$)[a], but-3-yn-l-en-2-yl | |
| | 1.50 | ($^1$**2**$^+$)[a] | |
| | 1.53 | ($^1$**3**$^+$)[a] | |
| | 1.67 | ($^3$**4**$^+$)[a] | |
| | 2.00 | ($^1$**5**$^+$)[a] | |
| | 2.03 | ($^3$**6**$^+$)[a] | |
| $C_4H_2^+$ | 0.00 | ($X^2\Pi$) | $\Delta_f H(C_4H_2^+) = 14.98$ eV[f] |
| | 2.44 | ($A^2\Pi$) | |
| | 6.44 | (B) | |

[a] Calculations in [23].
[b] Details of structures in [23].
[c] See Section 3.1 and [23,35].
[d] See Section 3.1 and [23,35–38].
[e] See Section 3.1 and [36–38].
[f] See Section 3.1 and [36,42,43].

ies of diacetylene at 2.44 eV ($A^2\Pi_u$) and 6.44 eV (B) above the ground state ($X^2\Pi_g$) [42–44] (Table 1).

### 3.2. Processes observed, reaction probabilities, and reaction exoergicities

In crossed-beam scattering experiments, two product ions were observed in collisions of the dication $C_4H_3^{2+}$ with the series of atoms and molecules, namely the cations $C_4H_3^+$ and $C_4H_2^+$. Their formation can be related to the following processes:

non-dissociative charge transfer

$$C_4H_3^{2+} + M \rightarrow C_4H_3^+ + M^+ \quad (1)$$

proton transfer

$$C_4H_3^{2+} + M \rightarrow C_4H_2^+ + MH^+ \quad (2)$$

dissociative charge transfer

$$C_4H_3^{2+} + M \rightarrow C_4H_2^+ + H + M^+ \quad (3)$$

The product ions $C_4H_3^+$ or $C_4H_2^+$ were scattered preferentially forward with respect to the direction of the incoming dication reactant (see further on). Therefore, the other reaction products, $M^+$ or $MH^+$, were scattered backwards, mostly into the experimentally inaccessible region backward in the laboratory frame of reference. The percent ratio of the products $C_4H_3^+/(C_4H_3^+ + C_4H_2^+)$ and $C_4H_2^+/(C_4H_3^+ + C_4H_2^+)$ was determined from measurements of the product ion intensities (lock-in signals) at the angular maximum.

The charge transfer process follows basically the "reaction window" concept even if molecular species are involved [45]. According to the reaction window concept, the charge transfer cross-section tends to be large, if the crossing between the reactant and (Coulomb repulsive) product potential energy surface occurs at internuclear distances that correspond to exoergicities of the processes, $\Delta E$, of about 2–5 eV [45–48]. The overall energy balance of a charge transfer process with molecular species is

$$E_{TOT} = T + E_{int} + \Delta E = T' + E'_{int} \quad (4)$$

where $T$ is the c.m. translational energy, $E_{int}$ the internal energy (vibrational and rotational) of the reactants, and $\Delta E$ is the exoergicity of the process, primed quantities refer to products. Therefore, a certain amount of energy can originate and/or be deposited as internal energy and thus the position of the relative translational energy maximum $\Delta T = T' - T$ may differ from the exoergicity of the process $\Delta E$. This energy difference can be mostly assigned to vibrational excitation due to the conformation change when going from reactants to the products and it was shown to follow basically the Franck–Condon vertical transition rules [45,49,50]. The change in rotational energy in dication–cation charge transfer processes was found to be quite small ("rotationally cold" products [45]).

The proton transfer reaction was found earlier to be an efficient channel in reactions of hydrogen-containing dication $CHCl^{2+}$ [17] and to proceed by an impulsive mechanism at the collision energy of about 2 eV.

Besides in the proton transfer reaction (2), the product ion $C_4H_2^+$ can be formed in a dissociative charge transfer reaction (3), if the internal energy of $C_4H_3^+$ exceeds the dissociation limit. The exoergicity of DCT reaction (3) is by 4.2 eV lower than the exoergicity of NDCT reaction (1) or by the dissociation energy of $MH^+$ to $M^+ + H$ lower that the exoergicity of reaction (2).

The reaction systems investigated and exoergicities of the reactions (1) and (2), for the series of the investigated target atoms and molecules (M = Kr, Xe, NO, $N_2$, $H_2$, $NH_3$, $C_2H_2$, and $CH_4$), are summarized in Table 2. The exoergicities were calculated for the ground states of the ions. In addition, Table 2

Table 2
Exoergicities, probabilities $P$(NDCT), $P$(PT), and relative integral cross-sections of non-dissociative charge transfer (NDCT) and proton transfer (PT) in the $C_4H_3^{2+}$ + M systems studied

| M | $T$ (eV) | IE(M)[a] (eV) | $\Delta E$(CT) (eV) | $\Delta_f H$(M)[a] (eV) | $\Delta_f H(MH^+)$[b] (eV) | $\Delta E$(PT) (eV) | $P$(NDCT) | $P$(PT) | $Q_R$ (a.u.) |
|---|---|---|---|---|---|---|---|---|---|
| Kr | 7.59 | 14.00[c] | 2.0 | 0 | 11.45 | 2.6 | 0.80 | 0.12 | 0.6 |
| | | 14.66[d] | 1.3 | | | | | | |
| Xe | 11.55 | 12.13[c] | 3.9 | 0 | 10.71 | 3.3 | 0.66 | 0.06 | 0.8 |
| | | 13.43[d] | 2.6 | | | | | | |
| NO | 5.85 | 9.26 | 6.7 | 0.946 | 11.11 | 3.9 | <0.04 | 0.04 | 0.58 |
| $NH_3$ | 4.00 | 10.16 | 5.8 | −0.48 | 6.55 | 7.0 | 0.32 | 0.52 | 0.92 |
| $C_2H_2$ | 3.3 | 11.40 | 4.6 | 2.36 | 11.53 | 4.9 | 0.31 | n.a. | |
| | 5.24 | | | | | | 0.34 | n.a.[e] | 0.97 |
| | 7.90 | | | | | | 0.34 | n.a.[e] | 1.00 |
| $CH_4$ | 3.80 | 12.51 | 3.5 | −0.77 | 9.37 | 3.9 | 0.90 | n.a.[e] | 0.46 |
| $N_2$ | 5.7 | 15.58 | 0.4 | 0 | 10.73 | 3.3 | <0.1 | n.a.[e] | 0.07 |
| $H_2$ | 0.64 | 15.42 | 0.6 | 0 | 11.47 | 2.6 | 0.2 | n.a.[e] | 0.06 |

[a] Ref. [38].
[b] Ref. [37].
[c] $^2P_{3/2}$.
[d] $^2P^{l/2}$.
[e] Data for net $P$(PT) not available.

lists ionization energies of M [38], heats of formation of the neutral species (M) [38], and of the protonated species $MH^+$ [37], used in the calculations of exoergicities. The table gives also information on collision (c.m.) energies of the crossed-beam experiments. The experiments were carried out at a similar laboratory translational energy of the reactant dication, close to 16 eV, and thus the collision energies in Table 2 differ considerably, depending on the mass of the target atom or molecule. An exception was the system with acetylene, studied more in detail at several collision energies.

Relative probabilities of the processes observed, non-dissociative charge transfer, $P$(NDCTA), proton transfer, $P$(PT), and dissociative charge transfer, $P$(DCT), were obtained from mass spectra of product ions measured in the beam scattering and in the mass spectrometric QOQ experiments. From the beam scattering experiments, the product ion ratio $I(C_4H_3^+)/[I(C_4H_3^+)+I(C_4H_2^+)]$ was obtained and from it $P$(NDCT). To complement the beam scattering data and to elucidate possible occurrence of the DCT reaction, a series of QOQ experiments was carried out. Mass spectra of the reactant and product ions were measured at two nominal reactant dication laboratory energies and the percent ratios of intensities of the reaction products $I(C_4H_3^+)/[I(C_4H_3^+)+I(C_4H_2^+)]$ and $I(MH^+)/[I(M^+)+I(MH^+)]$ were determined. The measurements were made only for reactions with Kr, Xe, NO, and $NH_3$. In the system with nitrogen, the exact ratio $I(N_2H^+)/[(I(N_2^+)+I(N_2H^+)]$ could not be determined because of a high background signal at $m/z$ 28. Nonetheless, proton transfer clearly dominates over charge transfer. The same conclusion comes from other guided-beam experiments.[3] For the system with acetylene (interference of the reactant ion intensity in the vicinity of $m/z$ 26.5) and methane the mass spectrometric QOQ data were not obtained. The fraction of DCT in these two cases had to be approximately estimated from the beam scattering experiments and the analysis of product translational energy distribution (see later on).

The ratio $I(C_4H_3^+)/[I(C_4H_3^+)+I(C_4H_2^+)]$ from the QOQ experiments turned out to be possibly influenced by collision-induced and spontaneous dissociation of highly internally excited projectile ions $C_4H_3^{2+}$ to $C_4H_2^+ + H^+$ along the long reactant ion beam path. On the other hand, this effect could be practically excluded in the single-collision crossed-beam scattering experiments (laboratory velocity of $C_4H_2^+$ from the collision-induced dissociation in the scattering center should be similar or smaller than the laboratory velocity of the reactant $C_4H_3^{2+}$ and could be easily distinguished). Therefore, for the ratio $I(C_4H_3^+)/[I(C_4H_3^+)+I(C_4H_2^+)]$ the value from the crossed-beam experiments was used. On the other hand, the ratio $I(MH^+)/[I(M^+)+I(MH^+)]$, inaccessible in the beam scattering experiments, was obtained from the QOQ experiments. The ratios of the three processes, non-dissociative charge transfer, $P$(NDCT), proton transfer, $P$(PT), and dissociative charge transfer, $P$(DCT), were then obtained as $P(\mathrm{NDCT}) = I(C_4H_3^+)/[I(C_4H_3^+)+I(C_4H_2^+)]$, $P(\mathrm{PT}) = I(MH^+)/[I(M^+)+I(MH^+)]$, and $P(\mathrm{DCT}) = 1 - P(\mathrm{NDCT}) - P(\mathrm{PT})$. The values of the measured intensity ratios are given in Table 2. The percent values of the relative probabilities are summarized in Fig. 2, plotted arbitrarily in dependence on the ionization energy of the target. In those cases, where the value for $P$(PT) (black columns) was not available from the QOQ measurements, only the sum of $P(\mathrm{PT}) + P(\mathrm{DCT}) = 1 - P(\mathrm{NDCT}) = I(C_4H_2^+)/[I(C_4H_3^+) + I(C_4H_2^+)]$ is given (cross-hatched columns).

The relative total cross-sections, $Q_R$, obtained from the mass spectra as a ratio between the sum of intensities of the two products, $I(C_4H_3^+)+I(C_4H_2^+)$, and the reactant ion intensity, $I(C_4H_3^{2+})$, $Q_R = [I(C_4H_3^+)+I(C_4H_2^+)]/I(C_4H_3^{2+})$, at the same

[3] R. Thissen, unpublished results.

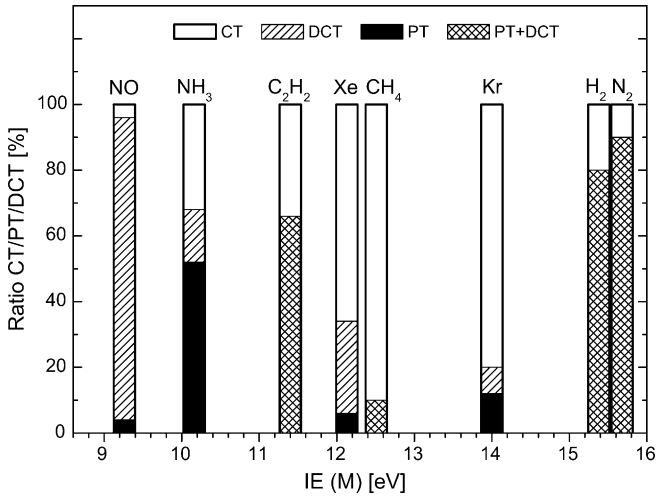


Fig. 2. Relative probabilities (%) of formation of non-dissociative charge transfer products (NDCT, open), dissociative charge-transfer products (DCT, hatched), and proton transfer products (PT, black) as estimated from crossed-beam and mass spectrometric tandem QOQ experiments for the studied reactions between $C_4H_3^{2+}$ and atoms and molecules. Only the sum of $P(PT) + P(DCT)$ is given (cross-hatched), if data for net $P(PT)$ are not available.

target gas pressure, are shown in the last column of Table 2. The relative cross-sections of reactions with $H_2$ and $N_2$ were substantially smaller (about 5–10 times) than for the other target molecules and very close to the detection limit. Therefore, the data for these reactions are only approximate.

### 3.3. Reactions with $C_2H_2$

First we describe the results for reactions with acetylene, as this system was studied more in detail, at several collision energies, and complete scattering diagrams of both products were obtained at a collision energy close to 3.4 eV. The QOQ data for this system could not be obtained due to an interference of the strong reactant ion signal ($m/z$ 25.5) at the product ion masses $M^+$ ($m/z$ 26) and $MH^+$ ($m/z$ 27). Therefore, the possible role of DCT has to be estimated from the available crossed-beam data.

Fig. 3 shows the scattering diagrams of the product ions $C_4H_3^+$ (a) and $C_4H_2^+$ (b) at the collision energy of 3.40 and 3.37 eV, respectively, together with the respective Newton diagrams. In the scattering diagrams in Fig. 3, the position of the center-of-mass is denoted by CM, the horizontal line shows the direction of the relative velocity. The scattering diagrams show a strongly forward-scattered product $C_4H_3^+$ ($C_4H_2^+$) with the peak of the distribution at the c.m. scattering angle 0° and at the center-of-mass velocity of the product ion of 2.75 km/s ($C_4H_3^+$) and 2.68 km/s ($C_4H_2^+$). At about 2.2 km/s, there is an indication of a smaller side peak in both scattering diagrams. Forward scattering of the charge transfer product is in agreement with earlier studies of charge transfer processes of dications [46,47].

Fig. 4 summarizes distributions of relative translational energy of the products, $P(T')$, for reactions leading to the products $C_4H_3^+ + C_2H_2^+$ (a) and $C_4H_2^+ + C_2H_3^+$ (b). For $T = 3.40$ (3.37) eV the $P(T')$ curves were obtained by the usual [25,26] integration of the entire scattering diagrams in Fig. 3a and b,

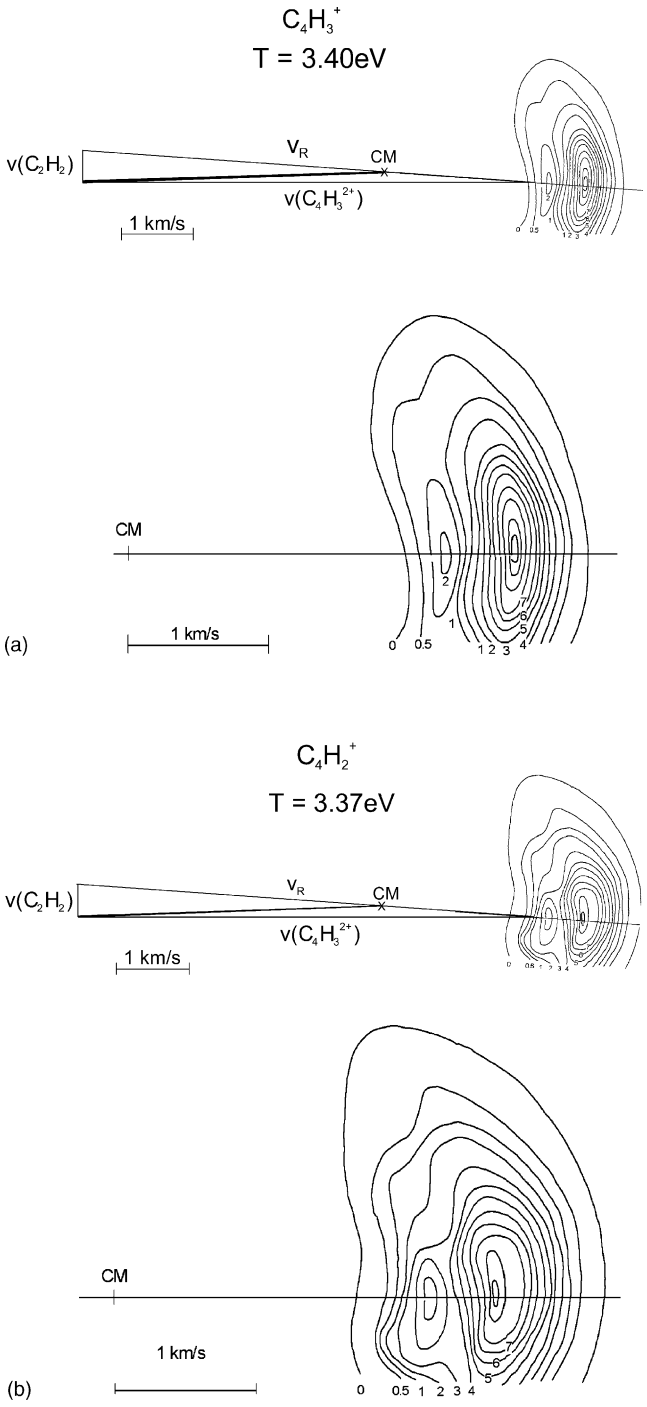


Fig. 3. $C_4H_3^{2+} + C_2H_2$: Newton diagrams and detailed contour scattering diagrams of $C_4H_3^+$ (a) and $C_4H_2^+$ (b) from the reaction at $T = 3.40$ eV (3.37 eV). Solid horizontal line denotes the direction of the relative velocity, CM marks the position of the tip of the velocity vector of the center-of-mass.

respectively. For $T = 5.24$ (5.30) and 7.90 eV the distributions were obtained from energy profiles at a laboratory angle close to the CM velocity vector. The profiles are plotted as a function of the relative translational energy of the products, $T'$ (upper scale), and of the reaction translational exoergicity, $\Delta T = T' - T$ (lower scale). The scales inside the figures indicate positions of exoergicities of the respective processes leading to the ground or excited states of the product ions.

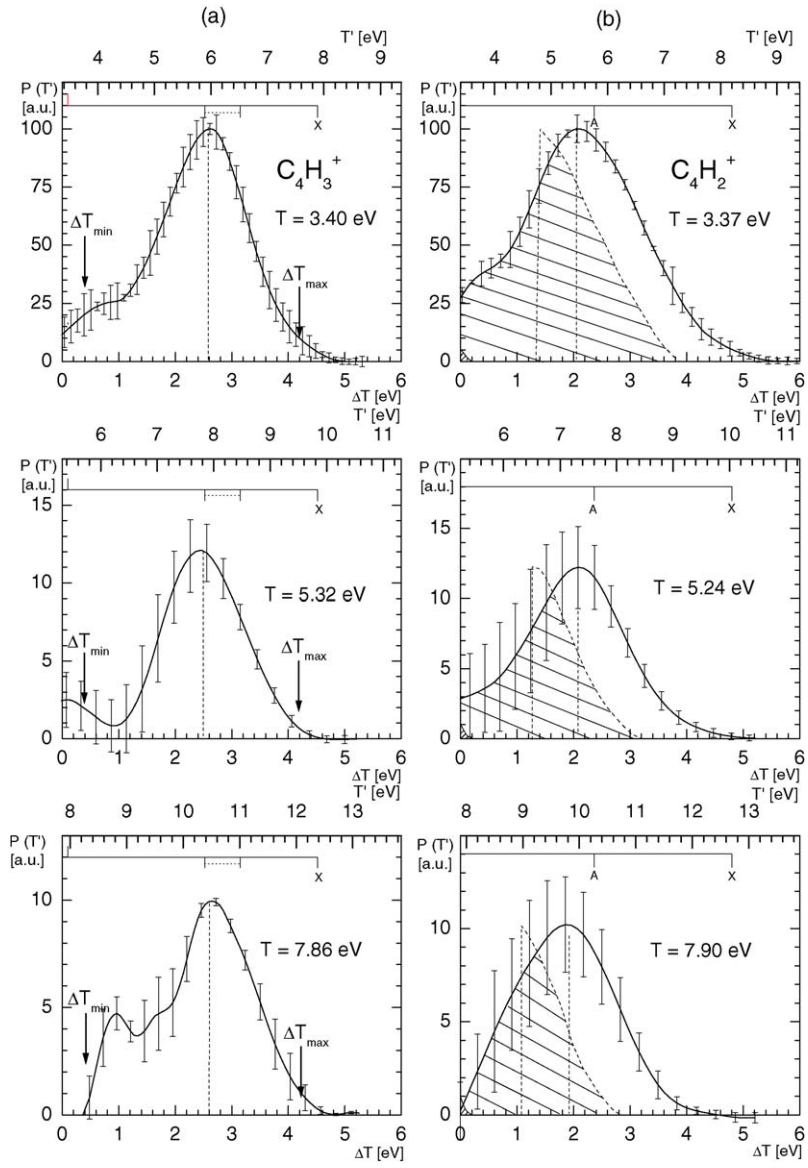


Fig. 4. $C_4H_3^{2+} + C_2H_2$: relative translational energy distributions, $P(T')$, of products of the NDCT reaction ($C_4H_3^+$ formation, a), and of the PT (including DCT) reaction ($C_4H_2^+$ formation, b) at several collision energies. The data are plotted against translational exoergicity $\Delta T = T' - T$ (lower scale) and $T'$ (upper scale). Horizontal scales indicate exoergicities of the processes in question (of the series of $C_4H_3^+$ excited states only the first and the last, connected by a dashed line, are shown). Hatched areas are the estimated regions, where DCT contributes to the formation of $C_4H_2^+$ for the two limiting cases of $E_{int}(C_4H_3^{2+})$, 0 and 3.8 eV. For the meaning of $(\Delta T)_{min}$ and $(\Delta T)_{max}$ see text.

The relative translational energy distributions for $C_4H_3^+ + C_2H_2^+$ at different collision energies peak very close to the same value of $\Delta T = T' - T = 2.7$ eV. The peak is about 1.9 eV lower in energy than the exoergicity of the NDCT reaction to ground state products $C_4H_3^+ + C_2H_2^+$ (4.6 eV). The energy difference of 1.9 eV between $\Delta E$ and $\Delta T$ should add to the internal (vibrational) energy excitation of the products. Another possibility is formation of the product $C_4H_3^+$ in the excited triplet state $^3\mathbf{1}^+$, 1.37 eV above the ground state (Table 1). Internal (vibrational) excitation of $C_4H_3^+(^3\mathbf{1}^+)$ from the NDCT process will be then $1.9 - 1.37 = 0.53$ eV. The ground state of the dication $C_4H_3^{2+}$ and both the ground state of the cation $C_4H_3^+(^1\mathbf{1}^+)$ and the excited triplet state $C_4H_3^+(^3\mathbf{1}^+)$ are linear and have a rather similar $H_2C–C–C–CH$ structure [23]. Thus, not much conformation change is expected in the vertical transition [45] connected with the charge transfer process $C_4H_3^{2+} \rightarrow C_4H_3^+$. In view of this, formation of the excited triplet state $C_4H_3^+(^3\mathbf{1}^+)$ and deposition of a rather small energy of 0.5 eV into the internal energy of the products seems to be more likely. We assume here that the other NDCT reaction product, $C_2H_2^+$, does not carry any substantial internal excitation; this assumption is reasonable, because the vertical transition $C_2H_2 \rightarrow C_2H_2^+$ is known to lead prevailingly to the vibrational ground state of $C_2H_2^+$ (see photoelectron spectra of acetylene [42]). The small peak at low $\Delta T$ of 0–1 may be connected with the formation of the ground state $C_4H_3^+$ and excited state of the other reaction product, $C_2H_2^{+*}$ (exoergicity about 0.2 eV).

The reaction product $C_4H_3^+$ can dissociate to $C_4H_2^+ + H$, if its internal energy is larger than 4.2 eV (see above). Thus, the reaction product $C_4H_3^+$ in Fig. 4a in the vicinity and below $\Delta T_{min} = (T' - T)_{min} = \Delta E + E_{int} - D = 4.6 - 4.2 = 0.4$ eV (arrow) should dissociate (see Eq. (4) for $(E_{int})_{min} = 0$ eV, and $E'_{int} = D(C_4H_3^+) = 4.2$ eV) and contribute to the formation of $C_4H_2^+$ in a DCT reaction, even if the initial internal energy of the dication reactant is zero. However, it appears likely that the initial internal energy of $C_4H_3^{2+}$ can be as high as close to the dissociation limit (see Section 3.1). For the maximum initial internal excitation, $(E_{int})_{max} = 3.8$ eV, the reaction product in Fig. 4a should dissociate, if $(\Delta T)_{max} = \Delta E + E_{int} - D = 4.6 + 3.8 - 4.2 = 4.2$ eV (arrow), i.e., practically over the entire range of $\Delta T$ of its formation (Fig. 4a). For the intermediate initial excitation of the reactant dication between the limits $0 < E_{int} < 3.8$ eV, the limiting $\Delta T$ for dissociation will decrease from 4.2 to 0.4 eV, but it will concern a substantial part of the region of $\Delta T$, over which we observe the formation of $C_4H_2$.

However, the nature of charge transfer processes of dications requires channeling of some of the energy available (see Eq. (4)) into the translational energy of the charge transfer products. In the case of the NDCT reaction with acetylene (Fig. 4a) its peak value is $(\Delta T)_{CT} = 2.6$ eV at all collision energies investigated. Therefore, the energy available for dissociation of the reaction product $C_4H_3^+$ will be accordingly lower than the dissociation limits $(\Delta T)_{min}$ and $(\Delta T)_{max}$, as discussed above. The respective regions, where the dissociation of the primary NDCT product $C_4H_3^+$ may contribute to the formation of $C_4H_2^+$, are shown in Fig. 5b by hatched areas (densely and loosely) for both limiting cases of $E_{int} = 0$ eV (close to $\Delta T = 0$ in Fig. 4b) and 3.8 eV, respectively. These regions were determined by subtracting from $(\Delta T)_{min}$ and $(\Delta T)_{max}$ the value of $(\Delta T)_{CT}$ and including the tailing of the $P(T')$ curves toward lower $T'$ (lower $T'$ means higher $E'_{int}$). It can be expected that the DCT product $C_4H_2^+$ will appear at the same velocities as the dissociating charge transfer product $C_4H_3^+$. Note, however, that the reduced masses of the proton transfer product pair, $C_4H_2^+ + C_2H_3^+$, and the DCT pair, $(C_4H_2^+ + H) + C_2H_2^+$, slightly differ and thus the scales of $T'$ and $\Delta T$ for these two product pairs are somewhat different. This was taken into account when hatched regions in Fig. 5b were determined. Thus, it seems that the initial internal energy of the dication reactant significantly influences the fraction of dissociative energy transfer. As we do not know the distribution of the initial internal energy of the dication, $P(E_{int})$, we can only make a reasonable guess about its role in the relative probability of the DCT versus the PT process.

The reasoning about the limiting cases of initial internal excitation of the reactant dication, as described above, leads us to the conclusion that a substantial fraction of the product $C_4H_2^+$ probably results from charge transfer followed by dissociation of the charge transfer product $C_4H_3^+$ (excited above its dissociation limit) to $C_4H_2^+ + H$, namely from the process

$$C_4H_3^{2+} + C_2H_2 \rightarrow C_2H_2^+ + C_4H_3^{+*} \rightarrow C_4H_2^+ + H + C_2H_2^+ \quad (5)$$

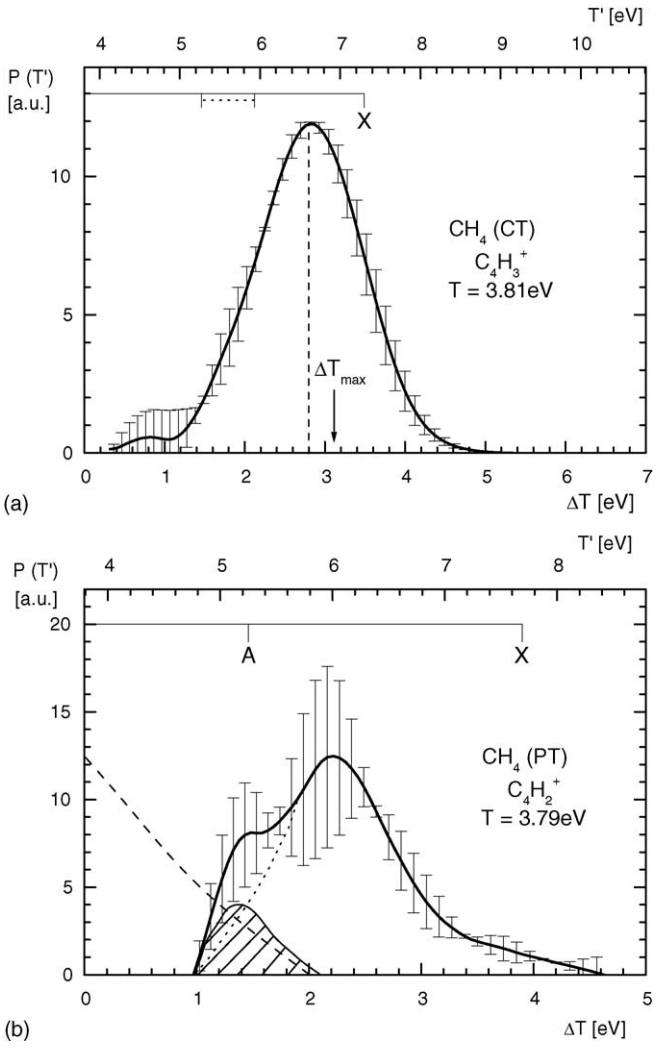


Fig. 5. $C_4H_3^{2+} + CH_4$: relative translational energy distributions, $P(T')$, of products of the NDCT reaction ($C_4H_2^+$ formation, a), and of the PT (including DCT) reaction ($C_4H_2^+$ formation, b) at $T = 3.81$ eV (3.79 eV), plotted against translational exoergicity $\Delta T = T' - T$ (lower scale) and $T'$ (upper scale). Horizontal scales indicate exoergicities of the processes in question. Data obtained from energy profiles measured at the laboratory scattering angle $\Theta_L = 2.0°$. Hatched area was obtained by subtracting from the $P(T')$ the hump at 1–2 eV. Dashed lines on the left indicate the region, where DCT can contribute to $C_4H_2^+$ formation, if $E_{int}(C_4H_3^{2+}) = 3.8$ eV. Other symbols are the same as in Fig. 4.

The contribution of the proton transfer reaction to the formation of $C_4H_2^+$ will be then correspondingly diminished. Evidently, the initial internal excitation of the projectile dication plays an important role in promoting the DCT process. Only in the unlikely case that it were zero or close to zero, one could expect that practically all (99%) of the $C_4H_2^+$ formed (see $P(T')$ curves for $C_4H_2^+$ in Fig. 4b, above $\Delta T$ of about 0.2 eV) could result from the proton transfer reaction. On the other hand, for the maximum initial internal energy of the dication, 3.8 eV, a large fraction of the $C_4H_2^+$ (about 50%) should result from DCT and the PT reaction should contribute to the formation of products $C_4H_2^+ + C_2H_3^+$ only in the upper part of the $P(T')$ curves for $C_4H_2^+ + C_2H_3^+$ for $\Delta T$ of 1.5–5 eV (unhatched area under the $P(T')$ curve in Fig. 4b). The reality is somewhere between these two limits. Any quantitative estimation is obviously quite diffi-

cult without a good knowledge of $P(E_{int})$. The proton transfer products are very probably formed in their ground states (X).

### 3.4. Reactions with $CH_4$

For reactions with methane the QOQ data are unfortunately not available, too. Only scattering data on relative probabilities of formation of $C_4H_3^+$ and $C_4H_2^+$ were obtained (Fig. 2). Thus, the fraction of $C_4H_2^+$ likely to be formed by DCT has to be approximately estimated, similarly as in reactions with acetylene. The data indicate prevailing NDCT ($C_4H_3^+$ formation) favored with respect to $C_4H_2^+$ formation by 9:1 (Fig. 2). The translational energy profiles of both $C_4H_3^+$ and $C_4H_2^+$ products were measured along a laboratory scattering angle close to the direction of the CM velocity vector and the results are given in Fig. 5a and b.

The $P(T')$ curve for the NDCT process (Fig. 5a) is rather narrow (FWHM less than 2 eV) and peaks at $\Delta T$ of 2.8 eV, about 0.6 eV below the exoergicity of the reaction to ground-state products $C_4H_3^+$ and $CH_4^+$. Therefore, it is very probable that both products are formed in their ground states, and the difference of about 0.6 eV between $\Delta E$ and $\Delta T$ adds to the internal excitation of the products. Such an internal excitation can be connected with the conformation change in forming the two products, namely in forming $CH_4^+$. Following the same argumentation as with the acetylene system, one can estimate that for the system with methane the values of $(\Delta T)_{min}$ and $(\Delta T)_{max}$ are −0.7 and 3.1 eV, respectively. The peak value of the relative translational energy of the NDCT products $(\Delta T)_{CT} = 2.8$ eV. Thus, the energy region in which the DCT reaction can occur, assuming maximum initial internal energy of the dication projectile $E_{int} = 3.8$ eV, is as indicated by the dashed line and hatched area of Fig. 5b. For the other extreme, $E_{int} = 0$ eV, the possible dissociation region is shifted much to the left, to negative values of $\Delta T$, and does not play a role. The hump in the $P(T')$ curve for $C_4H_2^+$ (Fig. 5b) may be connected with the contribution of the DCT reaction. However, a larger portion of the translational energy distribution of $C_4H_2^+$ should result from PT and formation of the products $C_4H_2^+ + CH_5^+$, both products most probably in their ground states. Accommodation of up to about 2.5 eV as internal energy of the two product ions should be possible.

### 3.5. Reactions with $NH_3$

Formation of both $C_4H_3^+$ and $C_4H_2^+$ was observed in this system, at $T = 4.0$ eV in a ratio of about 1:2 (Fig. 2). However, the combination of beam scattering and mass spectrometric QOQ data indicates that about 23% of the product $C_4H_2^+$ is formed by DCT (Table 2 and Fig. 2). Energy profiles of both hydrocarbon product ions were measured and the results are given in Fig. 6a and b.

The relative translational energy distribution, $P(T')$, for the NDCT process (formation of $C_4H_3^+ + NH_3^+$) exhibits a peak at $\Delta T$ of about 2.7 eV (Fig. 6a). This suggests that an excited state of the hydrocarbon cation $C_4H_3^+$ and the ground state of the $NH_3^+$ ion may be formed. The amount of 0–1.5 eV (peak value of 0.9 eV) can be expected to be confined to the internal

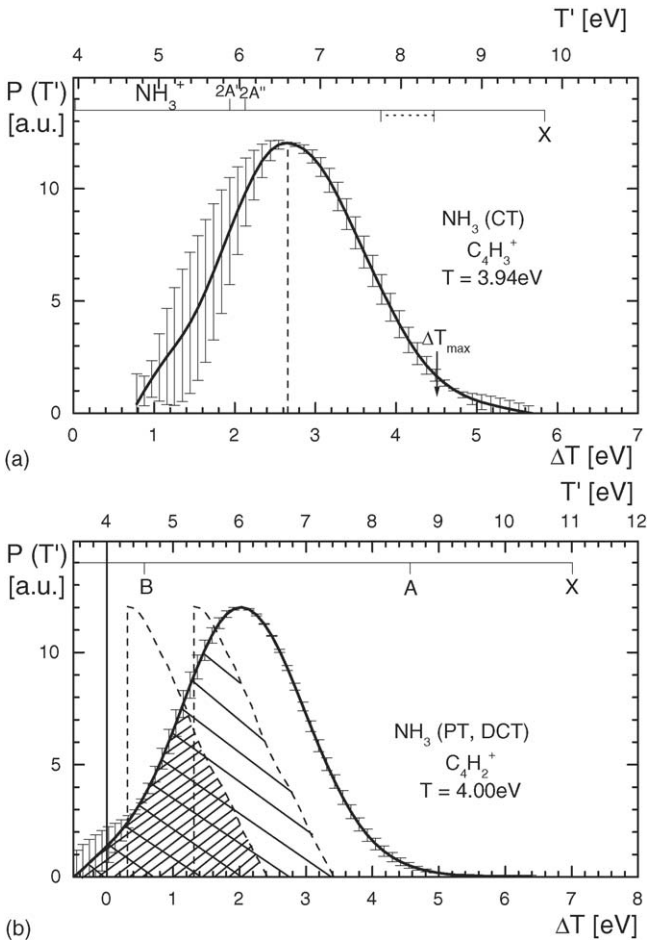


Fig. 6. $C_4H_3^{2+} + NH_3$: relative translational energy distributions, $P(T')$, of products of the NDCT reaction ($C_4H_3^+$ formation, a), and of the PT (including DCT) reaction ($C_4H_2^+$ formation, b) at $T = 3.94$ eV (4.00 eV), plotted against translational exoergicity $\Delta T = T' - T$ (lower scale) and $T'$ (upper scale). Horizontal scales indicate exoergicities of the processes in question. In the upper part, upward horizontal scale indicates exoergicities for formation of excited states of $NH_3^{+*}$. The hatched region indicates energy region, where dissociative charge transfer is likely to contribute to the formation of $C_4H_2^+$ for two different final states of $NH_3^+$ (see text). Data obtained from energy profiles measured at the laboratory scattering angle $\Theta_L = -1.5°$.

energy of the $NH_3^+$ product formed in the vertical ionization process [50]. Even so, the internal energy of the projectile dication would lead to dissociation of most of the NDCT product $C_4H_2^+$ (for the maximum $E_{int} = 3.8$ eV, $(\Delta T)_{max} = \Delta E + E_{int} - D - E'_{int}(NH_3^+) = 5.8 + 3.8 - 4.2 - 0.9 = 4.5$ eV, see the discussion above). Taking into account the energy channeled into $(\Delta T)_{CT}$ (peak value of 2.6 eV), the region of $C_4H_2^+$ from DCT would still occupy most of the area of $P(T')$ of $C_4H_2^+$ in Fig. 6b (loosely hatched area), leaving very little for formation of the proton transfer products.

Another possibility is that in the NDCT process the ground state of the hydrocarbon ion $C_4H_3^+$ is formed together with the excited, Jahn–Teller split state of $NH_3^{+*}$ (2A′ and 2A″). A substantial part of the energy available will be then confined to electronic excitation of $NH_3^+$ ($\Delta E = \sim 2.4$ eV). An approximate energy balance of this case indicates that only a part of the product $C_4H_2^+$ at low $\Delta T$ (0–2 eV) would result from DCT (densely

hatched in Fig. 6b for the maximum internal energy of the reactant dication, 3.8 eV). A larger part of the $C_4H_2^+$ product should be then formed in the proton transfer reaction (2), as observed in the experiment (Fig. 2). The long tailing of the $P(T')$ curve for the NDCT products in Fig. 6a indicates that the former process, formation of both charge transfer products in their ground states, may contribute partly to $C_4H_3^+$ formation at higher $\Delta T$ (2.5–5.5 eV).

The peak of the translational energy distribution of the proton-transfer products at 2 eV suggests that the hydrocarbon product is formed in the electronic excited state with considerable internal excitation. However, internal excitation of this amount could be confined in the two reaction products, $C_4H_2^+$ (A) and $NH_4^+$.

### 3.6. Reactions with NO

In the reaction with NO only formation of the product ion $C_4H_2^+$ could be detected in the crossed-beam experiments. The probability of the NDCT reaction was found to be less than a few percent and the value assigned to it came rather from the noise level of the signal. Therefore, the NDCT product $C_4H_3^+$ could not be measured. The combination of beam scattering and QOQ mass spectrometric results in Fig. 2 clearly show that the product $C_4H_2^+$ results mostly from dissociation of the charge transfer product and not from the proton transfer chemical reaction (very small amount of $HNO^+$ with respect to $NO^+$).

Fig. 7 shows the respective Newton diagram with the velocity distribution of the product ion $C_4H_2^+$ (upper part) and the product translational energy distribution (lower part) plotted against $\Delta T$ with $T'$ calculated for the putative DCT product pair $(C_4H_2^+ + H) + NO$ (upper scale, $T'_{DCT}$) and the proton-transfer pair $C_4H_2^+$–$HNO^+$ (lower scale, $T'_{PT}$). Following the preceding discussion, the values of $(\Delta T)_{min}$ and $(\Delta T)_{max}$, for the minimum and maximum initial internal excitation of the reactant dication, are 2.6 and 6.3 eV, respectively. Having in mind the peak energy of the translational energy distribution, 2.5 eV, the region in which the product of the NDCT reaction, $C_4H_3^+$, can dissociate is the densely hatched region between $\Delta T(C_4H_2^+$–$HNO^+)$ of 0.8–1.1 eV for the minimum initial internal energy excitation of the dication ($E_{int} = 0$ eV). For the maximum initial internal energy excitation, $E_{int} = 3.8$ eV, practically all product can dissociate (the limit is at 4.7 eV; see Fig. 7). Thus, it appears likely that the majority of the product $C_4H_2^+$ comes from DCT, namely from the reaction

$$C_4H_3^{2+} + NO \rightarrow NO^+ + C_4H_3^{+*} \rightarrow C_4H_2^+ + H + NO^+ \quad (6)$$

The proton transfer could possibly contribute to the distribution in the $\Delta T_{PT}$ region between 3 and 4 eV for initial internal excitation of the reactant dication $0 < E_{int} < 3.8$ eV (formation of ground-state proton transfer products).

The NDCT reaction to ground-state products has a very high exoergicity of 6.7 eV. The process should be out of the reaction window and should have only a small probability. However, formation of the NDCT hydrocarbon cation product $C_4H_3^+$ in the excited triplet state ($\Delta E = 5.4$ eV) should increase the probability

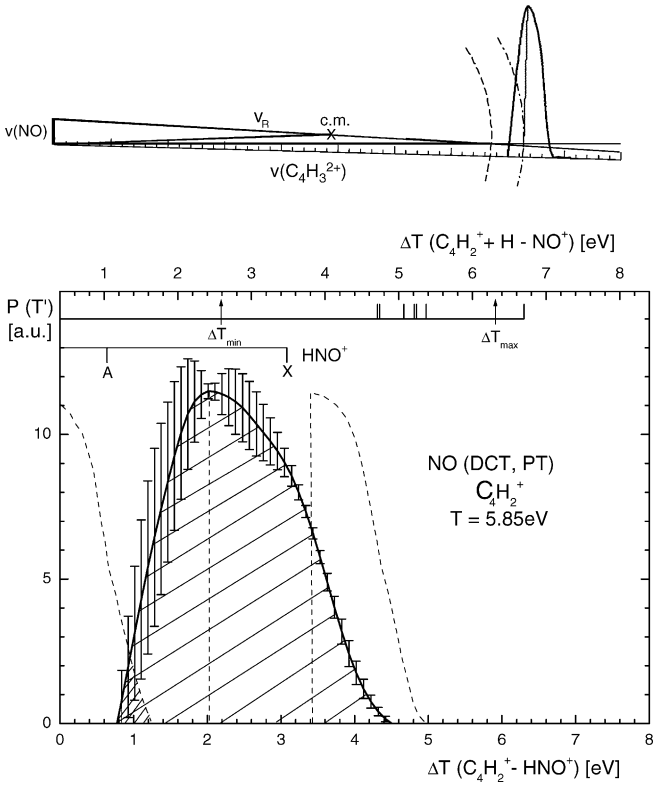


Fig. 7. $C_4H_3^{2+} + NO$: Newton diagram for collisions at $T = 5.85$ eV, the velocity profile of $C_4H_2^+$ measured at $\Theta_L = -1.5°$ (upper part), and the $P(T')$ curve obtained from it. The data are plotted against $\Delta T$ for the PT pair (lower scale) and for the DCT pair (upper scale). Symbols and hatched areas have the same meaning as in Fig. 4 (see text).

of its formation considerably. Also, formation of other excited states of the NDCT primary product $C_4H_3^+$ or (unknown) dissociative states of this cation, converging to the same limit at 10.17 eV (Fig. 1), may contribute to the reaction.

### 3.7. Reaction with Kr

In case of reactions with krypton, only the NDCT process was measured. The intensity of the $C_4H_2^+$ product was much smaller in the scattering experiments and the $P(T')$ curve could not be reliably determined. Estimation of $P(PT)$ from the QOQ mass spectrometric measurements suggests a considerable contribution of DCT to the formation of this product.

The respective $P(T')$ curve (Fig. 8, upper part) for the NDCT is characterized by two maxima. The lower-energy maximum at $\Delta T$ of 1.5 eV is very close to the exoergicity of the electron exchange process leading to the ground-state hydrocarbon cation $C_4H_3^+$ and the upper state of the $Kr^+$ spin–orbit doublet $^2P_{1/2}$ (1.3 eV). The more prominent, higher energy maximum, about twice as high, occurs at $\Delta T$ of 2.5 eV. The separation between the two maxima is 1.0 eV, by about 0.3 eV bigger than the separation of the two spin–orbit states of $Kr^+$ (0.66 eV). However, it is likely that the two maxima in the translational energy distribution of the products indicate formation of the product in the two spin–orbit states of $Kr^+$ ($^2P_{3/2}$ and $^2P_{1/2}$) and the difference of the exact position of the maxima is due to experimental inaccuracy. The

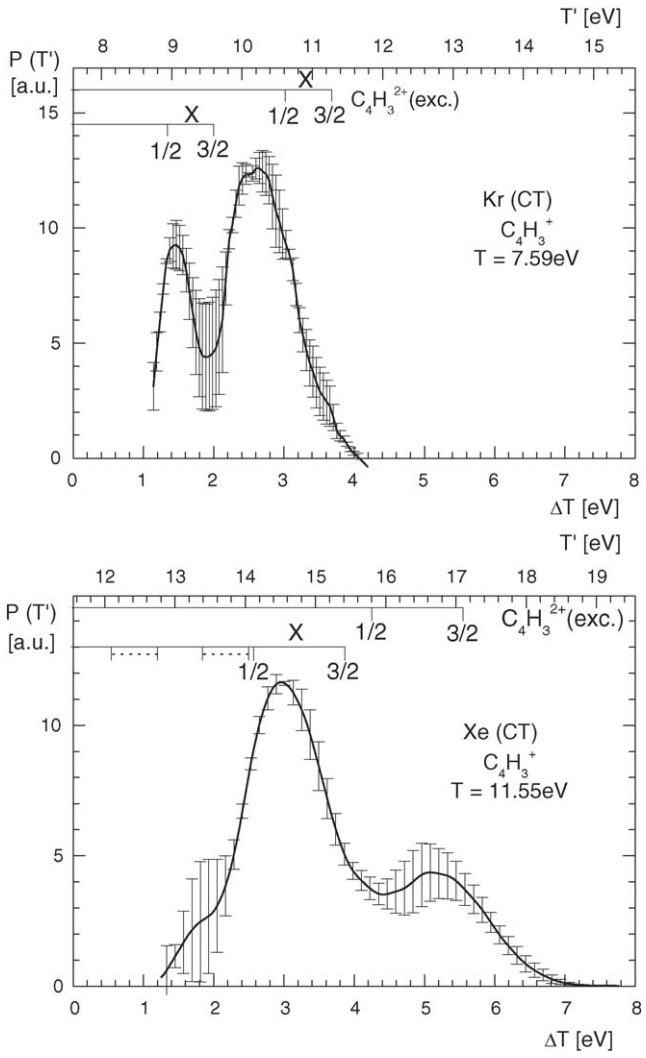


Fig. 8. $C_4H_3^{2+}$ Kr, Xe: relative translational energy distributions, $P(T')$, of products of the NDCT reaction ($C_4H_3^+$ formation) with Kr ($T = 7.59$ eV, upper part) and Xe ($T = 11.55$ eV, lower part) plotted against $\Delta T$ and $T'$. The horizontal scales refer to exoergicities of processes to different product states.

second scale in Fig. 8 shows exoergicities of the process with the excited state of the reactant dication. Participation of the excited reactant dication in the formation of the products may partly contribute to the $P(T')$ curve in Fig. 8 (upper part) at high $\Delta T$.

### 3.8. Reactions with Xe

Interaction with Xe at rather high collision energy of 11.55 eV leads to the formation of both products, with NDCT prevailing (Fig. 2). However, the mass spectrometric QOQ data for $P$(PT) indicate a large contribution of DCT to the product ion $C_4H_2^+$ formation (Table 2; Fig. 2) Unfortunately, for technical reasons, the translational energy distribution of the product ion $C_4H_2^+$ could not be determined and only beam scattering data for the NDCT channel are available. The $P(T')$ curve of the NDCT products $C_4H_3^+ + Xe^+$ in Fig. 8 (lower part) shows a prominent peak at $\Delta T$ of 3 eV, very close to the exoergicity of the reaction leading to the ground state of $C_4H_3^+$ and the upper state of the spin–orbit doublet of $Xe^+$, $^2P_{1/2}$ (2.6 eV). The $P(T')$ curve then exhibits a shoulder to higher translational energy with a peak (about 40% of the main peak) at 4.8–5.2 eV. The separation between the overlapping peaks, 1.8–2.2 eV, is larger than the spin–orbit splitting in $Xe^+$ (1.3 eV). However, it seems that both states of $Xe^+$ are formed, the $Xe^+(^2P_{1/2})$ with a higher probability due to a better position in the reaction window. The excited state of the reactant dication, 1.8 eV above the ground state (Table 1), may contribute to the formation of the products at $\Delta T$ of 5–6 eV.

### 3.9. Reactions with $N_2$ and $H_2$

In both cases the reaction cross-section was considerably smaller than with the other systems and thus only approximate data could be obtained. Most of the product ions come from the proton transfer process (80–90%; see Table 2). The reason for a negligible cross-section of the NDCT reaction is understandable: high ionization energy of both $N_2$ and $H_2$ makes the exoergicity of NDCT reaction with the ground state dication reactant below 1 eV and thus the process is rather improbable. Vibrational excitation of the dication reactant may influence the electronic part of the problem only through a change in the position of the crossings of the potential energy surfaces of the reactant and product systems. A small fraction of NDCT products observed presumably comes from an admixture of excited states $(C_4H_3^{2+})^*$ in the reactant beam.

With the nitrogen molecule as a target, only the more probable reaction of proton transfer could be measured at $T = 5.68$ eV (Fig. 9). Repeated many-scan recordings of the $C_4H_2^+$ energy distribution curves led to the $P(T')$ distribution shown in Fig. 9. The $P(T')$ curve suggests formation of both the ground state and the excited A-state of the hydrocarbon cation product $C_4H_2^+$, with a broad internal energy distribution.

The reaction with hydrogen was in a way unique in the series of investigated systems, as the collision energy was much smaller

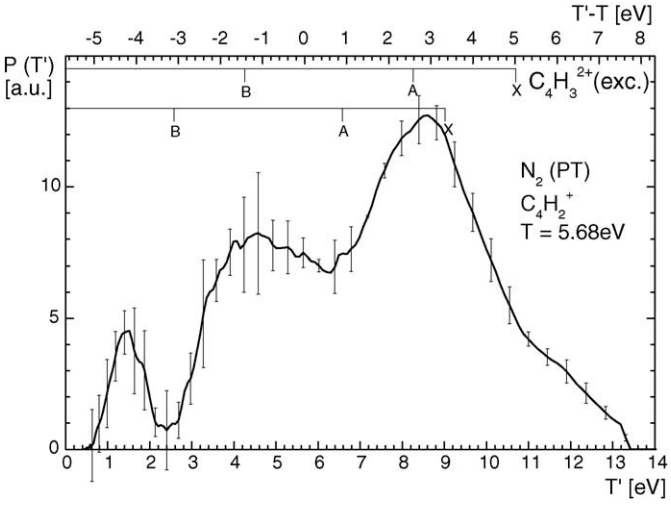


Fig. 9. $C_4H_3^{2+} + N_2$: relative translational energy distributions, $P(T')$, of products of the PT transfer reaction ($C_4H_2^+$) at $T = 5.68$ eV, plotted against translational exoergicity $\Delta T = T' - T$ (lower scale) and $T'$ (upper scale). Horizontal scales indicate exoergicities of the processes in question. Data obtained from energy profiles measured at the laboratory scattering angle $\Theta_L = 2.0°$.

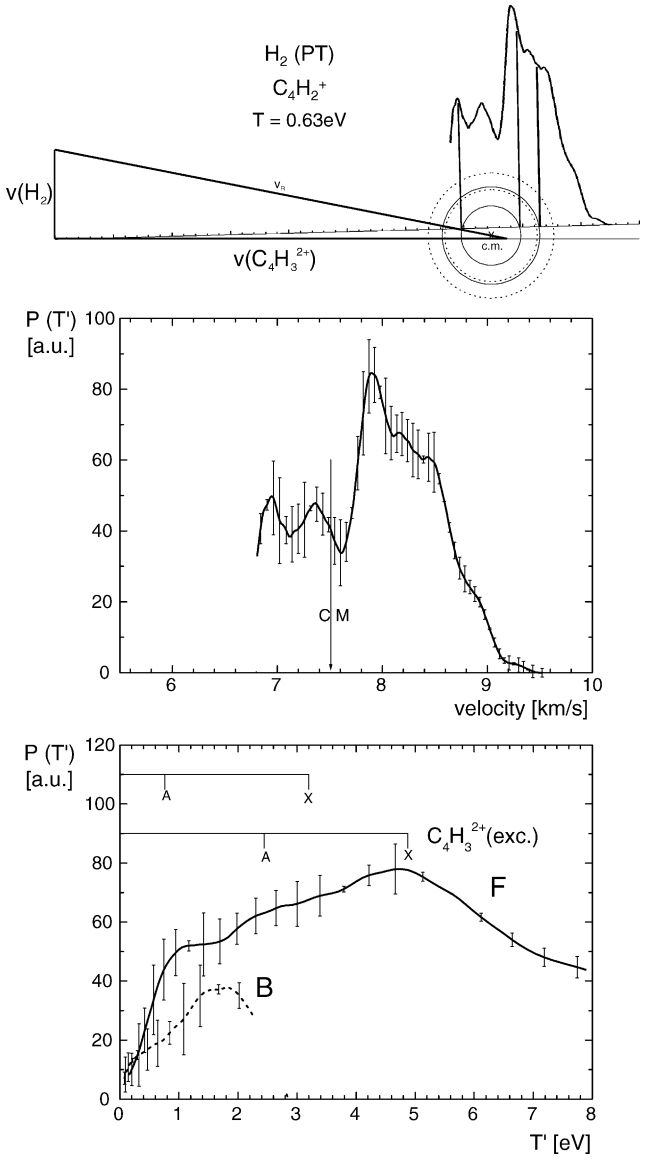


Fig. 10. $C_4H_3^{2+} + H_2$: data on the reaction product $C_4H_2^+$ from collisions at $T = 0.63$ eV. *Upper part*: Newton diagram with the velocity profile of $C_4H_2^+$; full circles indicate loci for formation of the X and A states of $C_4H_2^+$ in reaction with ground state $C_4H_3^{2+}$, dashed circles the same for reactions with excited $C_4H_3^{2+}$. *Middle part*: The velocity profile of $C_4H_2^+$ from the Newton diagram plotted against laboratory velocity of $C_4H_2^+$. *Lower part*: The respective $P(T')$ curve, plotted against $T'$ for the proton transfer product pair (F, forward scattered; B, backward scattered).

(0.63 eV). Only proton transfer reaction could be measured, as the total cross-section was – similarly as with $N_2$ – very small. The translational energy distribution of the product $C_4H_2^+$ was measured at the laboratory scattering angle of +1.5°, close to the direction of $v_{CM}$ and recalculated to the velocity distribution of $C_4H_2^+$. The results are shown in Fig. 10 (upper part) (Newton diagram and $C_4H_2^+$ velocity distribution). The velocity distribution shows product intensity tightly concentrated both forward and backward with respect to the center-of-mass of the system. This suggests formation of an intermediate at this low collision energy. Circles indicate exoergicities of the processes leading to ground state and excited products $C_4H_2^+ + H_3^+$ with the ground state (solid circles) and electronically excited (dashed) reactant dication. The relative translational energy distribution of the products is shown in Fig. 10 (lower part). The curve is not very informative, as the recalculation to $P(T')$ smears out the velocity distribution. Because of the unfavorable ratio of the product ion masses (50:3), the heavy ion $C_4H_2^+$ has a small c.m. velocity and the $P(T')$ curve is considerably affected by the velocity spread in the reactant ion beam. However, it may be concluded from the product velocity distribution and from the $P(T')$ distribution that the hydrocarbon product $C_4H_2^+$ is formed both in the ground (X) and excited (A) states, with a possible participation of the reaction from the excited state of the reactant.

### 3.10. Summarizing remarks

In retrospect, using a thermodynamically stable dication as the dication reactant seems to be about the worst choice. This dication may carry substantial initial internal energy, as the range of internal energies extends from the value given by the thermodynamic stability with respect to its dissociation limit, $E_D$, plus the Coulomb barrier connected with this limit, $E_B$ (schematic curves in Fig. 11, case 1). On the other hand, metastable dications are characterized by a lower Coulomb barrier toward an exoergic dissociation limit. Thus, only the dications with a rather small internal energy will survive to be involved in subsequent reactions (case 2, Fig. 11). An extreme in this case seems the

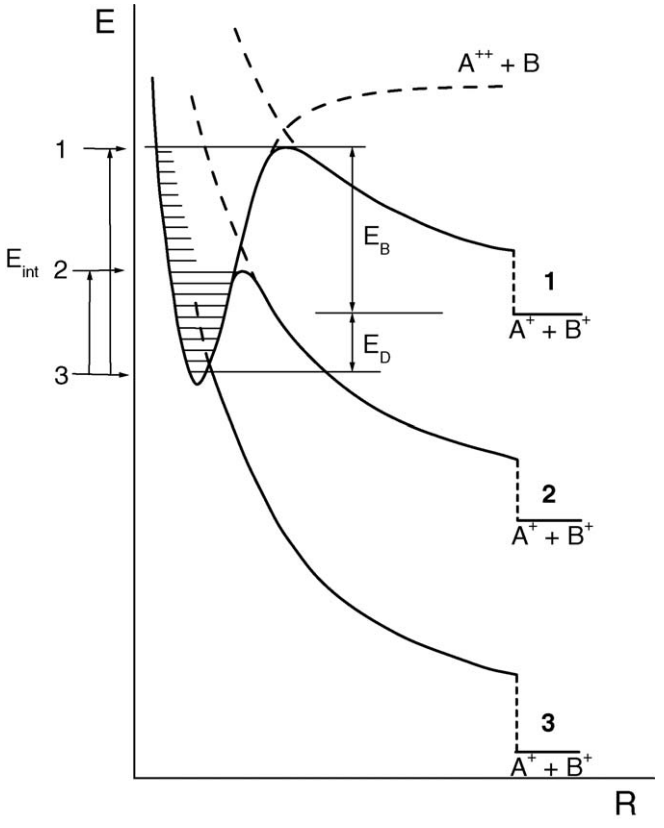


Fig. 11. Schematics of potential energy curves for thermodynamically stable and metastable molecular dications, effect on internal energy of the reactant dication, $E_{int}$.

dication $CO^{2+}$, where experiments indicate that practically only the ground vibrational states of the two lowest electronic states are non-dissociative [45–47] (case 3, Fig. 11). As this study shows, initial internal excitation of the reactant dication may play a significant role in determining the branching between charge transfer (both NDCT and DCT) and proton transfer processes.

## 4. Conclusions

1. Reactions of the hydrocarbon dication $C_4H_3^{2+}$ were investigated with a series of atoms (Kr and Xe) and molecules ($C_2H_2$, $CH_4$, $NH_3$, NO, $N_2$, and $H_2$) using the crossed-beam scattering method and tandem (quadrupole–octopole–quadrupole) mass spectrometric technique.
2. Formation of $C_4H_3^+$ in non-dissociative charge transfer reaction (1)

$$C_4H_3^{2+} + M \rightarrow C_4H_3^+ + M^+$$

and formation of $C_4H_2^+$ both in proton transfer (2)

$$C_4H_3^{2+} + M \rightarrow C_4H_2^+ + MH^+$$

and in dissociative charge transfer reaction (3)

$$C_4H_3^{2+} + M \rightarrow C_4H_2^+ + H + M^+$$

was observed. Relative probabilities of these reactions at the laboratory energy of $C_4H_3^{2+}$ of 16 eV were determined for the systems studied from results of both experimental methods.
3. In reactions with acetylene, scattering diagrams were measured for both products $C_4H_3^+$ and $C_4H_2^+$. The results showed preferential forward scattering, implying a direct, impulsive mechanism of the processes. A substantial part of the $C_4H_2^+$ appears to be formed in a dissociative charge transfer reaction; this is presumably due to a high initial internal energy content of the reactant dication $C_4H_3^{2+}$. The proton transfer reaction may contribute to the $C_4H_2^+$ product formation at higher values of the $P(T')$ distribution and the product is likely to be formed in its ground state.
4. In reactions with $CH_4$, formation of both $C_4H_3^+$ (non-dissociative charge transfer) and $C_4H_2^+$ (proton transfer) led to ground state products. In reactions with $NH_3$, the main channel was formation of $C_4H_2^+$, both in a proton transfer and (to a lesser extent) dissociative charge transfer reaction. In reactions with NO, only formation of $C_4H_2^+$ could be measured; this ion resulted mostly from the dissociative charge transfer reaction. Only a small part resulted from the proton transfer reaction.
5. Non-dissociative charge transfer reactions with noble gases Kr and Xe led to the ground-state product $C_4H_3^+$ and the noble gas cations $Kr^+$ or $Xe^+$ in both spin–orbit states.
6. In comparison with other studied reactions the reactions with $N_2$ and $H_2$ had a rather small relative cross-section (5–10 times) and led mostly to $C_4H_2^+$ formed in proton transfer reactions.

## Acknowledgements

Partial support of this research by the funds of the European Network "Generation, Stability and Reaction Dynamics of Multiply-Charged Ions" (MCInet), by the Association Euratom IPP.CR, and by the grant KJB4040302 of the Grant Agency of the Academy of Sciences is gratefully acknowledged. The authors thank H. Schwarz and D. Schröder, Berlin, for the allocation of measurement time on their multipole instrument, supported by a generous grant of the Deutsche Forschungsgemeinschaft.

## References

[1] K.G. Spears, G.C. Fehsenfeld, M. McFarland, E.E. Ferguson, J. Chem. Phys. 56 (1972) 2562.
[2] R. Tonkyn, J.C. Weisshaar, J. Am. Chem. Soc. 108 (1986) 7128.
[3] Y.A. Ranasinghe, T.M. MacMahon, B.S. Freiser, J. Phys. Chem. 95 (1991) 7721.
[4] J.C. Weisshaar, Acc. Chem. Res. 26 (1993) 231, and references cited therein.
[5] L.M. Roth, B.S. Freiser, Mass Spectrom. Rev. 10 (1991) 303.
[6] S.D. Price, M. Manning, S.R. Leone, J. Am. Chem. Soc. 116 (1994) 8673.
[7] Z. Dolejšek, M. Fárník, Z. Herman, Chem. Phys. Lett. 235 (1995) 99.
[8] Z. Herman, J. Žabka, Z. Dolejšek, M. Fárník, Int. J. Mass Spectrom. 192 (1999) 191.
[9] K.A. Newson, S.D. Price, Chem. Phys. Lett. 269 (1997) 93.
[10] N. Tafadar, D. Kearney, S.D. Price, J. Chem. Phys. 115 (2001) 8819; N. Tafadar, S.D. Price, Int. J. Mass Spectrom. 223–224 (2003) 547; N. Lambert, N. Kaltsoyannis, S.D. Price, J. Žabka, Z. Herman, J. Phys. Chem. A (2005), ASAP, doi:10.1021/jp052981d.
[11] L. Mrázek, J. Žabka, Z. Dolešek, J. Hrušák, Z. Herman, J. Phys. Chem. 104 (2000) 7294.
[12] S.W. Buckner, J.R. Gord, B.S. Freiser, J. Chem. Phys. 91 (1989) 7530.
[13] W. Lu, P. Tosi, D. Bassi, J. Chem. Phys. 112 (2000) 4648.
[14] D.K. Bohme, Can. J. Chem. 77 (1999) 1453.
[15] J. Roithová, J. Žabka, J. Hrušák, R. Thissen, Z. Herman, J. Phys. Chem. A 107 (2003) 7347.
[16] J. Roithová, J. Hrušák, Z. Herman, J. Phys. Chem. A 107 (2003) 7355.
[17] J. Roithová, R. Thissen, J. Žabka, P. Franceschi, O. Dutuit, Z. Herman, Int. J. Mass Spectrom. 228 (2003) 487.
[18] J. Roithová, J. Žabka, R. Thissen, Z. Herman, Phys. Chem. Chem. Phys. 5 (2003) 2988.
[19] E.R. Williams, J. Mass Spectrom. 31 (1995) 831.
[20] S.A. McLuckey, J.L. Stephenson, Mass Spectrom. Rev. 17 (1998) 369.
[21] S. Petrie, G. Javahery, H. Wincel, D.K. Bohme, J. Am. Chem. Soc. 115 (1993) 6290.
[22] B.E. Jones, L.E. Abbey, H.L. Chatham, A.W. Hanner, L.A. Teleshefsky, E.M. Burgess, T.F. Moran, Org. Mass Spectrom. 17 (1982) 10.
[23] D. Schröder, J. Loos, H. Schwarz, R. Thissen, J. Roithová, Z. Herman, Int. J. Mass Spectrom. 230 (2003) 113.
[24] D. Schröder, H. Schwarz, J. Phys. Chem. A 103 (1999) 7385.
[25] B. Friedrich, Z. Herman, Coll. Czech Chem. Commun. 49 (1984) 570.
[26] Z. Herman, Int. J. Mass Spectrom. 212 (2001) 413.
[27] J. Roithová, D. Schröder, T. Weiske, P. Grüne, H. Schwarz, J. Phys. Chem. A (2005), ASAP, doi:10.1021/jp0545288.
[28] D. Becke, J. Chem. Phys. 84 (1986) 4524; D. Becke, J. Chem. Phys. 98 (1993) 1372; D. Becke, J. Chem. Phys. 98 (1993) 5648.
[29] C. Lee, W. Yang, R.G. Parr, Phys. Rev. B 37 (1988) 785.
[30] D.E. Woon, T.H. Dunning Jr., J. Chem. Phys. 98 (1993) 1358.

[31] R.A. Kendall, T.H. Dunning Jr., R.J. Harrison, J. Chem. Phys. 96 (1992) 6796.
[32] T.H. Dunning Jr., J. Chem. Phys. 90 (1989) 1007.
[33] M.J. Frisch, G.W. Trucks, H.B. Schlegel, G.E. Scuseria, M.A. Robb, J.R. Cheeseman, V.G. Zakrzewski, J.A. Montgomery Jr., R.E. Stratmann, J.C. Burant, S. Dapprich, J.M. Millam, A.D. Daniels, K.N. Kudin, M.C. Strain, O. Farkas, J. Tomasi, V. Barone, M. Cossi, R. Cammi, B. Mennucci, C. Pomelli, C. Adamo, S. Clifford, J. Ochterski, G.A. Petersson, P.Y. Ayala, Q. Cui, K. Morokuma, P. Salvador, J.J. Dannenberg, D.K. Malick, A.D. Rabuck, K. Raghavachari, J.B. Foresman, J. Cioslowski, J.V. Ortiz, A.G. Baboul, B.B. Stefanov, G. Liu, A. Liashenko, P. Piskorz, I. Komaromi, R. Gomperts, R.L. Martin, D.J. Fox, T. Keith, M.A. Al-Laham, C.Y. Peng, A. Nanayakkara, M. Challacombe, P.M.W. Gill, B. Johnson, W. Chen, M.W. Wong, J.L. Andres, C. Gonzalez, M. Head-Gordon, E.S. Replogle, J.A. Pople, Gaussian 98 (Revision A.11.4), Gaussian, Inc., Pittsburgh, PA, 2001.
[34] L.A. Curtiss, K. Raghavachari, G.W. Trucks, J.A. Pople, J. Chem. Phys. 94 (1991) 7221.
[35] J. Roithová, D. Schröder, J. Loos, H. Schwarz, H.-Ch. Jankowiak, R. Berger, R. Thissen, O. Dutuit, J. Chem. Phys. 122 (2005) 094306.
[36] J.H. Kiefer, S.S. Sidkin, R.D. Kern, K. Xie, H. Chen, L.B. Harding, Combust. Sci. Technol. 82 (1992) 101.
[37] E.P. Hunter, S.G. Lias, J. Phys. Chem. Ref. Data 27 (1998) 413.
[38] S.G. Lias, J.E. Bartmess, J.F. Liebman, J.L. Holmes, R.D. Levin, W.G. Millard, J. Phys. Chem. Ref. Data 17 (Suppl. 1) (1988) 1.
[39] R. Thissen, J. Delwiche, J.-M. Robbe, D. Duflot, J.-P. Flament, J.H.D. Eland, J. Chem. Phys. 99 (1993) 6590.
[40] D. Duflot, J.-M. Robe, J.-P. Flament, Chem. Phys. 102 (1995) 355.
[41] X. Li, B. Schlegel, J. Phys. Chem. A 108 (2004) 468.
[42] D.W. Turner, C. Baker, A.D. Baker, C.R. Brundle, Molecular Photoelectron Spectroscopy, Wiley/Interscience, London, 1980, p. 194.
[43] J.P. Maier, F. Thommen, J. Chem. Phys. 73 (1980) 5616.
[44] J. Lecoulter, J.P. Maier, M. Roesslein, J. Chem. Phys. 89 (1988) 6081.
[45] A. Ehbrecht, N. Mustafa, Ch. Ottinger, Z. Herman, J. Chem. Phys. 105 (1996) 9833.
[46] Z. Herman, Int. Rev. Phys. Chem. 15 (1996) 299.
[47] Z. Herman, Phys. Essays 13 (2000) 480.
[48] R.K. Janev, H. Winter, Phys. Rep. 117 (1985) 267.
[49] M. Fárník, Z. Herman, T. Ruhaltinger, J.P. Toennies, R.G. Wang, Chem. Phys. Lett. 206 (1993) 376.
[50] M. Fárník, Z. Herman, T. Ruhaltinger, J.P. Toennies, J. Chem. Phys. 103 (1995) 3495.